para-Sulfonated Calixarenes Used as Synthetic Receptors for Complexing Photolabile Cholinergic Ligand

by **Alexandre Specht**[a]), **Fabio Ziarelli**[b]), **Philippe Bernard**[c]), **Maurice Goeldner**[a]), and **Ling Peng***[d])

[a]) Laboratoire de Chimie Bioorganique, CNRS UMR 7514, Faculté de Pharmacie, Université Louis Pasteur Strasbourg, BP 24, F-67401 Illkirch Cedex

[b]) Spectropole, Universités Aix-Marseille I et III, Faculté des Sciences et Techniques de St. Jérôme, Avenue Escadrille Normandie-Niemen, F-13397 Marseille Cedex 13

[c]) GREENPHARMA S. A., 3 Allée du Titane, F-45100 Orléans

[d]) Département de Chimie, CNRS UMR 6114, Université Aix-Marseille II, 163, Avenue de Luminy, F-13288 Marseille Cedex 9 (phone: 0033 491 82 91 54; fax: 0033 491 82 93 01; e-mail: ling.peng@univmed.fr)

The water-soluble tetra-, hexa- and octasulfonated calix[4]arenes, calix[6]arenes, and calix[8]arenes **1**–**3**, respectively, were investigated as potential synthetic receptors for photolabile cholinergic ligand **A**, a photolytic precursor of choline. Ligand **A** is a bifunctional molecule carrying a photolabile 2-nitrobenzyl group at one end and a choline moiety at the other end. Results from NMR studies have shown that calixarenes **1**–**3** form stable 1:1 complexes with **A**, having similar binding potential to that observed with the cholinergic enzymes acetylcholinesterase and butyrylcholinesterase. Further studies have suggested that calix[8]arene forms a ditopic complex by binding concomitantly to both the cationic choline moiety and the aromatic photolabile group of **A**, whereas calix[4]arene and calix[6]arene form monotopic complexes with **A**. The ditopic complex between calix[8]arene and **A** results from mutually induced fitting process, while the monotopic complexes between calix[4]arene and **A** can be regulated by pH: at neutral pH, calix[4]arene specifically binds the cationic choline moiety, while, at acidic pH, it complexes unselectively both the cationic choline moiety and the aromatic group of **A**. Our results show that *para*-sulfonated calixarenes are versatile artificial receptors which bind in various ways to the bifunctional photolabile cholinergic ligand **A**, depending on their size, geometry, and state of protonation.

Introduction. – Molecular recognition is a fundamental biological process that has inspired many chemists to design artificial receptors and enzymes [1]. Among them, the calixarene family is of special importance. Calixarenes are macrocylic molecules consisting of phenolic units connected at the *ortho*-position by CH_2 bridges. There exist many conformational isomers of calixarenes, and a large number of cavities of different sizes and shapes, which can be involved in molecular recognition processes [2]. Various calixarene-based synthetic receptors have been developed [3], including the water-soluble tetra-, hexa-, and octasulfonated calix[4]arene, calix[6]arene, and calix[8]arenes **1**–**3**, respectively, which have attracted particular attention because they are able to host the neurotransmitter acetylcholine and related cholinergic ligands, and can, therefore, be used as synthetic cholinergic receptors [4][5]. The binding of cholinergic ligands to calixarenes is a complex process in which electrostatic forces, hydrophobic effects, and cation–π interactions [6] all play a crucial role. Our interest in developing photolabile cholinergic ligands [7–11] as possible means to photoregulate the activity of their biological hosts led us to investigate their interactions with calixarenes **1**–**3** as model receptors.

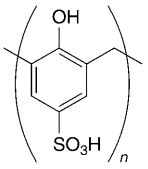

1 $n = 4$
2 $n = 6$
3 $n = 8$

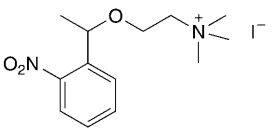

A

The photolabile cholinergic ligand **A** is a bifunctional molecule, which has a photolabile 2-nitrobenzyl group at one end and a choline moiety at the other end [7]. Upon photoactivation, **A** releases choline. Ligand **A** has been originally developed for time-resolved studies on cholinesterases (ChEs) such as acetylcholinesterase (AChE) and butyrylcholinesterase (BuChE) to reach a better understanding of their underlying functional mechanisms [8]. Meanwhile, water-soluble calixarenes can be used as synthetic receptors for this photolabile cholinergic ligand, yielding supramolecular host–guest systems which often mimic the molecular recognition features of the original biological molecules at a very basic level, and providing valuable information about the biological processes involved.

Our preliminary studies showed that calix[4]arene forms host–guest complexes with **A** by specifically binding to the ammonium groups at neutral pH [12], while calix[8]arene forms complexes with **A** by ditopically binding to both the cationic ammonium moiety and the aromatic ring *via* a mutually induced fitting process [13]. To gain more insight into these complexes, we have carried out detailed studies on the binding behaviour of calixanenes **1**–**3** with **A**.

Results and Discussion. – *Complex* [**A**-**1**]. In our previous report [12], we have showed, by NMR titration, that calix[4]arene (**1**) and ligand **A** formed a stable complex at neutral pH, with the quaternary ammonium group of **A** being specifically included in the cavity of **1**. We demonstrated here again, by Diffusion-Ordered Spectroscopy (DOSY)-NMR experiments, that **A** and **1** formed a stable complex. A DOSY experiment yielded a 2D spectrum (*Fig. 1*) with NMR chemical shifts in one dimension and diffusion coefficients in the other one. DOSY Experiments can, therefore, serve to distinguish compounds or complexes in terms of the differences in their diffusion rates [14]. With individual solutions in phosphate buffer, we obtained from DOSY experiments diffusion coefficients of 5.50×10^{-10} and 3.02×10^{-10} m^2/s for of **A** and **1**, respectively (*Fig. 1*). When mixed with **1**, **A** showed a significant decrease in the diffusion rate (2.88×10^{-10} m^2/s) in comparison with its free solution (*Fig. 1* and *Table 1*), indicating that **A** formed a complex with **1**. This is in agreement with the assumption that formed complexes diffuse slower. Therefore, the results of the DOSY experiments provided additional evidence that **A** and **1** formed a stable complex. It is to be mentioned here that the signals of the CH_2 bridges in **1** are absent in the DOSY spectrum of the complex [**A**-**1**]. This is caused by a processing artifact of the broad signals of the CH_2 bridges in **1**. These broad signals are characteristic of **1**, due to a slow conformational equilibrium at room temperature. For the calixarenes with larger rings, the equi-

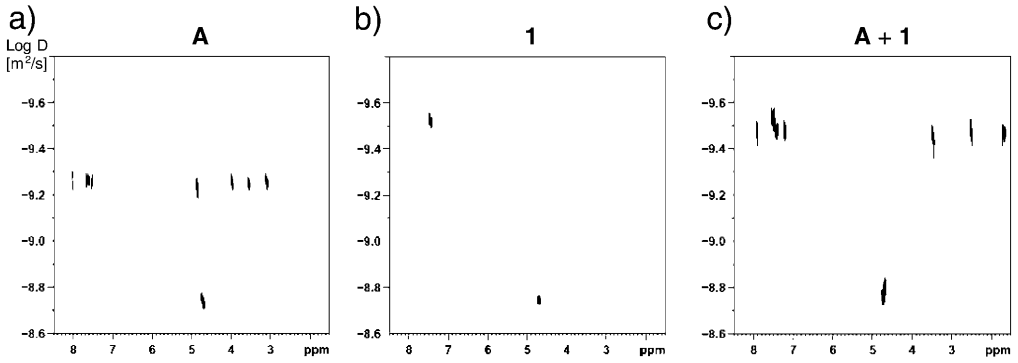

Fig. 1. *2D-DOSY Spectra recorded in* 0.1M *deuterated phosphate buffer, pD 7.3 at 300 K with* a) *ligand* **A**; b) *calix[4]arene* (**1**), c) **A** *and* **1** *in a* 1:1 *ratio*

Table 1. *Relative Diffusion Coefficients of the Free Calixarenes* **1**–**3** *and the Calixarene Complexes Formed with* **A** *in 100 mM Phosphate Buffer pD 7.3 at 300 K, and Estimated Molecular Weights* (M_r) *of the Calixarene Complexes Deduced from the DOSY Experiments.* The difussion coefficient of **A** is 5.50×10^{-10} m^2/s.

Calixarene	Diffusion coefficient of free calixarene [10^{-10} m^2/s]	Diffusion coefficient of calixarene complex [10^{-10} m^2/s]	Estimated M_r of complex	Theoretical M_r of complex
1	3.02	2.88	900	984
2	2.34	2.24	1300	1350
3	2.24	2.14	1700	1727

librium is faster, and, as a consequence, the signals of the CH_2 bridges will be sharp (see *Fig. 5* and *Fig. 6*) [15].

We established further the stoichiometry of the complex [**A**-**1**] by MS analyses, *Job*'s plot, and estimated molecular weight of complex. Electrospray MS analyses showed clearly that 1:1 complex was formed between **A** and **1** (*Fig. 2*,*a*). The *Job*'s plot obtained from the NMR analyses indicated the predominant formation of 1:1 complex between **A** and **1** (*Fig. 2*,*b*). Moreover, from the differences of the diffusion coefficients between the free calixarene **1** and the calixarene complex [**A**-**1**] in DOSY experiments, we deduced the molecular weight of [**A**-**1**] [16], which matched perfectly the theoretical molecular weights of the 1:1 complex for [**A**-**1**] (*Table 1*). Therefore, all the above results support the 1:1 stoichiometry for [**A**-**1**].

In [12], we reported that only the ammonium moiety of **A** was included in the cavity of **1** at neutral pH (*Fig. 3*,*a*) [12]. In the present study, we show that, at acidic condition, both the aromatic group and the ammonium moiety of **A** displayed important upfield chemical shifts, which reached saturation at large excess of **1** (*Fig. 4*). These results suggest that both the aromatic group and the ammonium moiety of **A** were included in the cavity of **1**. The binding of the ammonium moiety was only marginally affected by the pH, while the inclusion of the aromatic group became important at pD values ranging from 7.3 to 0.4 (*Table 2*). We know that the inclusion of the ammonium group of **A** in the cavity of **1** is driven mainly by the electrostatic interactions between the ammonium

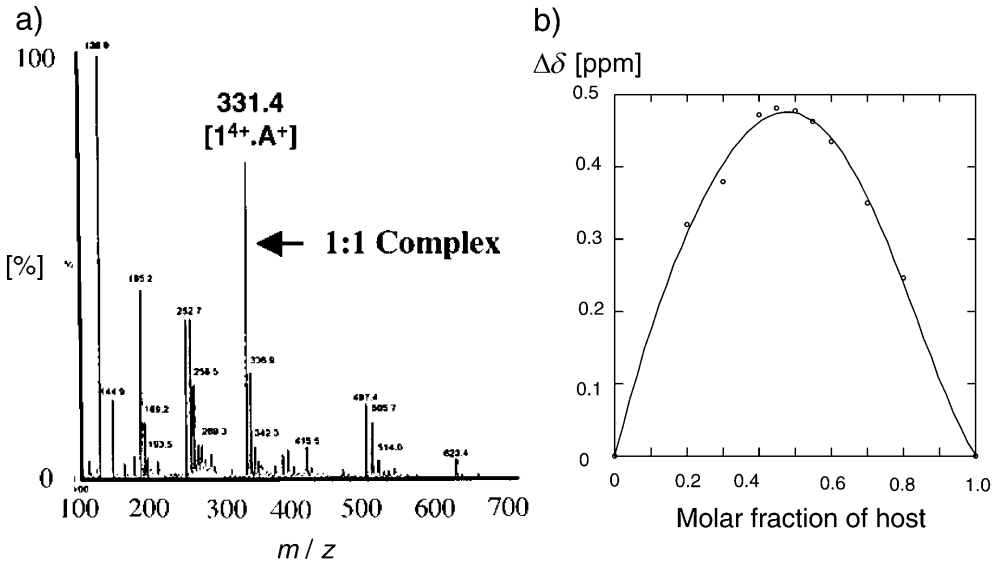

Fig. 2. a) *Mass-spectroscopic analysis and* b) Job's *plot of the complex* [**A**-**1**]

group of **A** and the sulfo groups in **1**, and the cation–π interactions between the cationic ammonium group of **A** and the aromatic units of **1** [17]. The change of pD from 7.3 to 0.4 will not influence signicifantly these interactions. Therefore, no important change for the inclusion of the ammonium group of **A** in **1** was observed when pD was changed from 7.3 to 0.4. However, the inclusion of the aromatic group of **A** in **1** is mainly driven by hydrophobic interactions. At pD 7.3, the OH groups of the phenol units in **1** are mainly deprotonated, favorable for eletrostatic interactions, but not for hydrophobic interactions, generating unfavorable conditions for complexing the aromatic ring of **A** in the cavity of **1** and leading to the specific inclusion of the cationic ammonium moiety, while at pD 0.4, the OH groups of phenol units in **1** are predominantly in nondissociated form, which favors hydrophobic interactions and aromatic π–π interactions. Therefore, at pD 0.4, the aromatic ring of **A** can be also favorably included in the cavity of **1**, and this inclusion is competing with that of the ammonium moiety, resulting in non-specific inclusion of both the ammonium moiety and the aromatic group.

Table 2. *^{1}H-NMR Maximum Upfield Chemical Shifts* ($\Delta\delta$, [ppm]) *and Dissociation Constants* (K_D, [μM]) *for the Ammonium Moiety and the Aromatic Ring in* **A** *When Complexed with* **1** *in 100 mM Phosphate Buffer at both pD 7.3 and pD 0.4*

pD	Me_3N^+		H–C(4) of Ar	
	$\Delta\delta_{max}$ [ppm]	K_D [μM]	$\Delta\delta_{max}$ [ppm]	K_D [μM]
7.3	1.79	68 ± 3	0.13	N.d.[a])
0.4	1.29	60 ± 9	1.19	190 ± 40

[a]) N.d.: Not determined

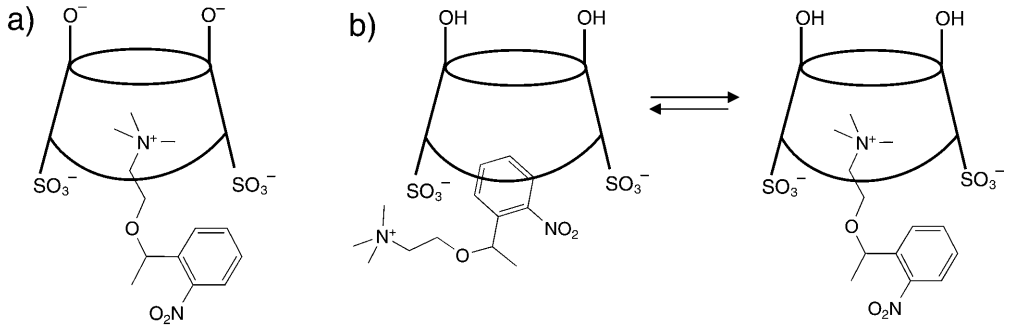

Fig. 3. *Monotopic binding complexation of* **1** *with* **A** *at* a) *pD 7.3 and* b) *pD 0.4*

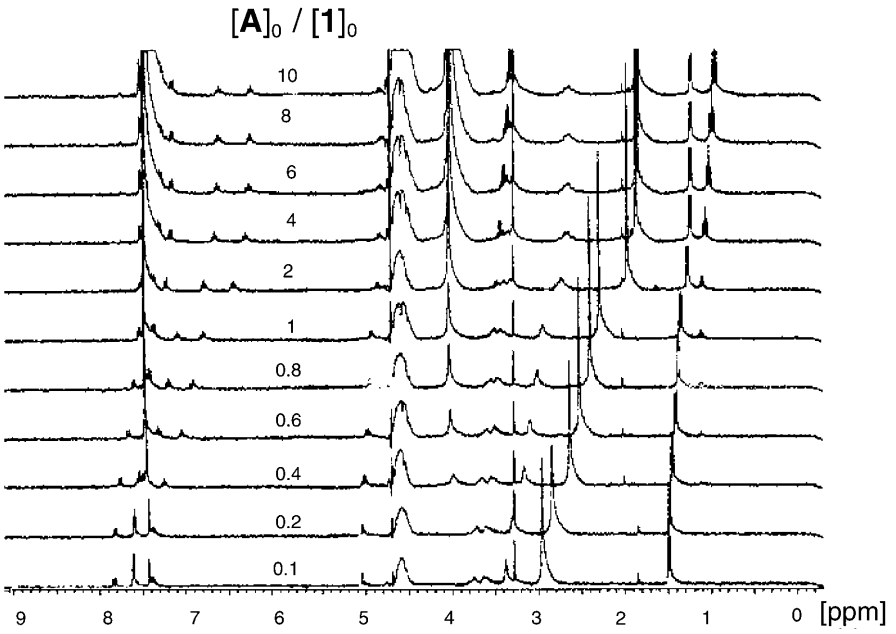

Fig. 4. *NMR Titration of the calix[4]arene* **1** *with* **A** *in 100 mM phosphate buffer at pD 0.4.* $[\mathbf{A}]_0$ and $[\mathbf{1}]_0$ are initial concentrations of **A** and **1**, resp.

Since both the aromatic ring and the ammonium moiety of **A** can be included in the cavity of **1** at pD 0.4, and the cavity of **1** is too small to accommodate both of them simultaneously, we propose a fast equilibrium between two monotopic complexes at pD 0.4 (*Fig. 3,b*). This binding mode correlates with the observed pH effect. This is also in line with the results published by *Shinkai et al.* [18] on the effects of the pH on the complexation of trimethylanilinium with **1**. The complexation of **1** with **A** can be, therefore, regulated by the pH.

Complex [**A**-**2**]. Similar to **1**, the calix[6]arene (**2**) forms stable complex with **A** at neutral condition as shown by NMR titration (*Fig. 5*) and DOSY experiments

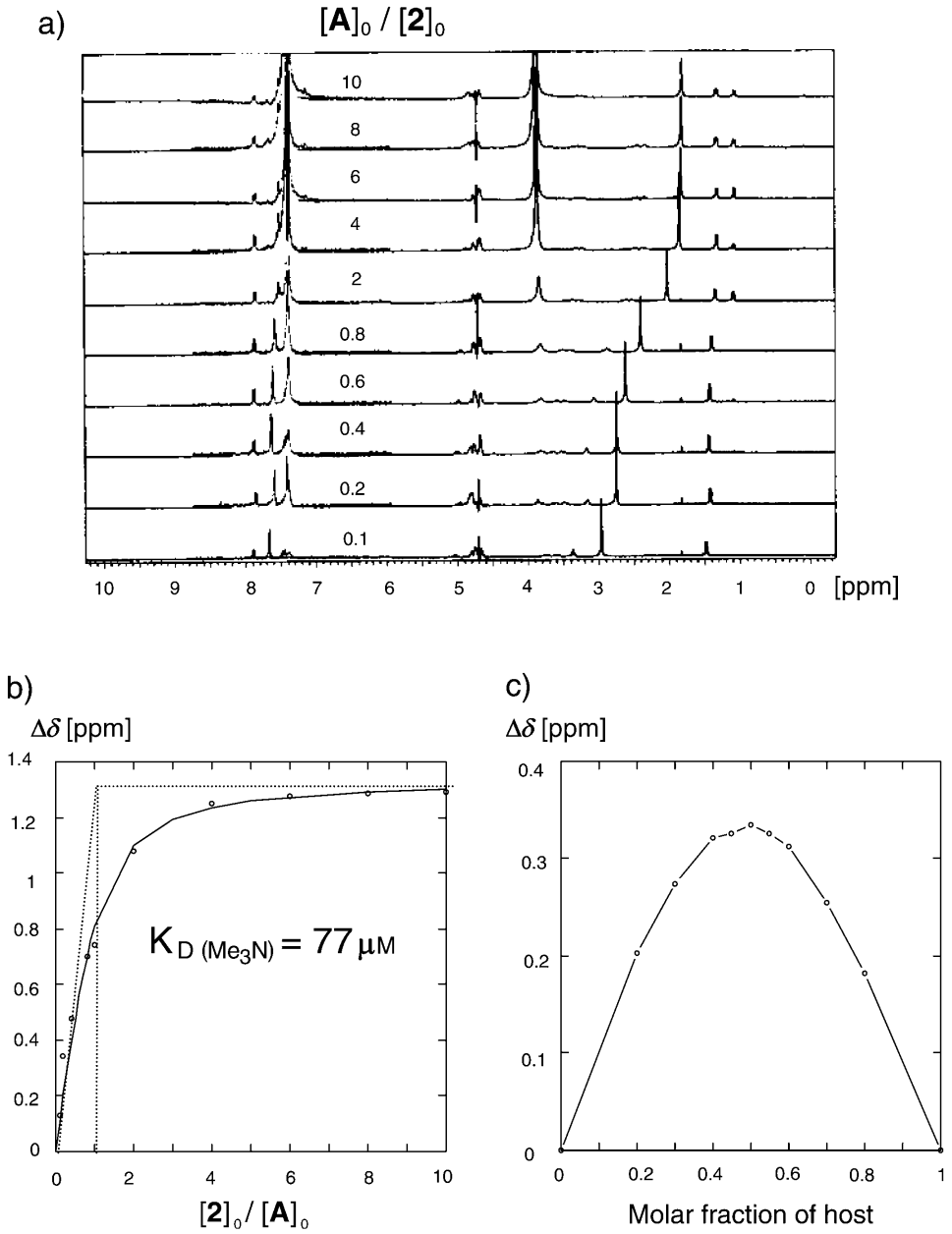

Fig. 5. a) *NMR Titration of the calix[6]arene* **2** *with* **A** *in 100 mM phosphate buffer at pD 7.3*. b) *Non-least squares fitting of NMR titration data for* [**A**-**2**]. c) *Job's plot of* [**A**-**2**]. $[\mathbf{A}]_0$ *and* $[\mathbf{2}]_0$ *are initial concentrations of* **A** *and* **2**, *respectively.*

(*Fig. 6*). In the NMR titration, the gradual addition of **2** to a buffered solution of **A** led to an increasing upfield shift ($\Delta\delta$) of the Me groups of the quaternary ammonium in **A**, which reached saturation when **2** was in large excess (*Fig. 5*). No change or only slight shift for the signals of the aromatic H-atoms was observed. This suggests the specific inclusion of the ammonium moiety of **A** in the cavity of **2**. In addition, the single and sharp NMR signal corresponding to the Me group of the ammonium moiety in **A** (*Fig. 5, a*), when complexed with **2**, indicated that a fast exchange had occurred between complexed and uncomplexed ligands on the NMR time scale.

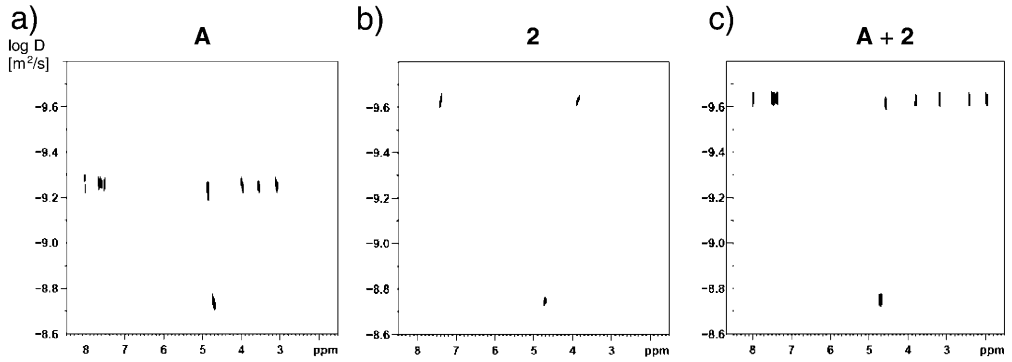

Fig. 6. *2D-DOSY Spectra recorded in* 0.1M *deuterated phosphate buffer, pD 7.3 at 300 K with* a) *ligand* **A**, b) *calix[6]arene* **2**, *and* c) **A** *and* **2** *in a 1:1 ratio*

For [**A**-**2**], we could not establish its stoichiometry by electrospray MS analyses, because the MS results were not informative due to the formation of multiply charged, complex ions. Nevertheless, the signals in DOSY experiments (*Fig. 6*) allowed us to deduce the estimated molecular weight of [**A**-**2**] (*Table 1*), which satisfactorily matched the theoretical molecular weights of the 1:1 host–guest complexes. In addition, *Job*'s plot confirmed unambigously the 1:1 stoichiometry for [**A**-**2**] (*Fig. 5, c*).

The stability of [**A**-**2**] was further assessed by determing its dissociation constant, obtained by performing non-linear least-squares fitting with the titration curves $\Delta\delta = f$[Calixarene]/[Ligand] [19], which gave a perfect match with a 1:1 bimolecular complex (*Fig. 5, b*). The dissociation constant for the complex [**A**-**2**] is around 77 μM, similar to that obtained for [**A**-**1**] (*Table 3*, below). Considering the cavity size of **2** and the above results, we conclude that [**A**-**2**] has a similar binding mode as [**A**-**1**].

Complex [**A**-**3**]. Our previous results of NMR titration experiments showed that **3** and **A** formed a stable complex by simultanious inclusion of both the aromatic ring and the choline moiety of **A** in the cavity of **3**, and that the complex [**A**-**3**] was of stoichiometry 1:1 [13]. Here, we confirmed further the formation of complex [**A**-**3**] by DOSY experiments (*Fig. 7*). Furthermore, we deduced the estimated molecular weight of [**A**-**3**] [16] (*Table 1*) from the diffference of diffusion coefficients between the free calixarene **3** and the calixarene complex [**A**-**3**]. The deduced molecular weight of [**A**-**3**] is in line with the theoretical molecular weight of the 1:1 complex for [**A**-**3**] (*Table 1*).

Table 3 contains the dissociation constants of the complexes formed between calixarenes **1**–**3** and **A**. These values were calculated from the chemical shifts of the quater-

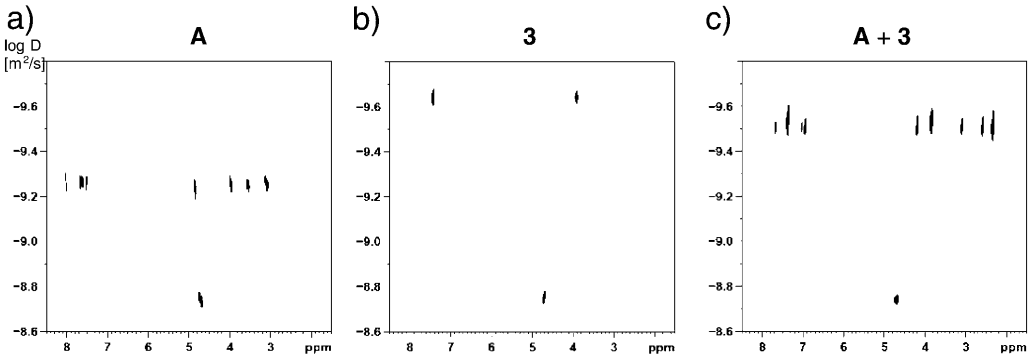

Fig. 7. *2D-DOSY Spectra recorded in* 0.1M *deuterated phosphate buffer, pD 7.3 at 300 K with* a) *ligand* **A**, b) *calix[8]arene* **3**, *and* c) **A** *and* **3** *in a 1:1 ratio*

Table 3. *Dissociation Constants* (K_D, [μM]) *of* **A** *Complexed with Calixarenes* **1**–**3** *in 100* mM *Phosphate Buffer at pD 7.3, in Comparison with Their Inhibition Constants* (K_I, [μM]) *Involved in the Binding Process with Acetylcholinesterase and Butyrylcholinesterase* [13]

K_D (**1**) [μM]	68 ± 3
K_D (**2**) [μM]	77 ± 21
K_D (**3**) [μM]	29 ± 10
K_I (Acetylcholinesterase) [μM]	13
K_I (Butyrylcholinesterase) [μM]	11

nary ammonium group of **A** in the complexes formed with **1** and **2**, and from the chemical shifts of both the quaternary ammonium and the aromatic H-atoms of **A** in the complex [**A**-**3**] [19]. The inhibitory constants (K_I) of **A** binding to AChE and BuChE [7], two important cholinergic enzymes, were also listed in *Table 3*. The dissociation constants of the various calixarene complexes ranged from 29 to 77 μM. The strongest interactions were observed with the complex [**A**-**3**], where the dissociation constants were similar to those observed with AChE and BuChE (*Table 3*). These findings suggest that the *para*-sulfonated calixarenes bind strongly to **A**, mimicking the binding sites of cholinesterases.

In view of the large annular cavity and the above findings, two possible modes of complexation between **A** and **3** can be postulated (*Fig. 8*). The first possibility is that both the quaternary ammonium moiety and the aromatic ring of **A** may be simultaneously complexed in the cavity of **3**, forming a ditopic binding complex (*Fig. 8,a*). The second possibility is that a fast equilibrium may be set up between two monotopic complexes, each of which hosts either the quaternary ammonium or the aromatic part of **A** (*Fig. 8,b*).

To deduce the binding mode involved in the complex [**A**-**3**], NMR titration was performed under neutral (pD 7.3) and acidic conditions (pD 0.4). When the pD changed from 0.4 to 7.3, neither the upfield chemical shift nor the dissociation constant was significantly affected for either the ammonium group or the aromatic moiety of **A** (*Table 4*). Although different chemical shifts were observed for the ammonium group and the aromatic ring in **A**, very similar binding constants were obtained (*Table 4*), based on the

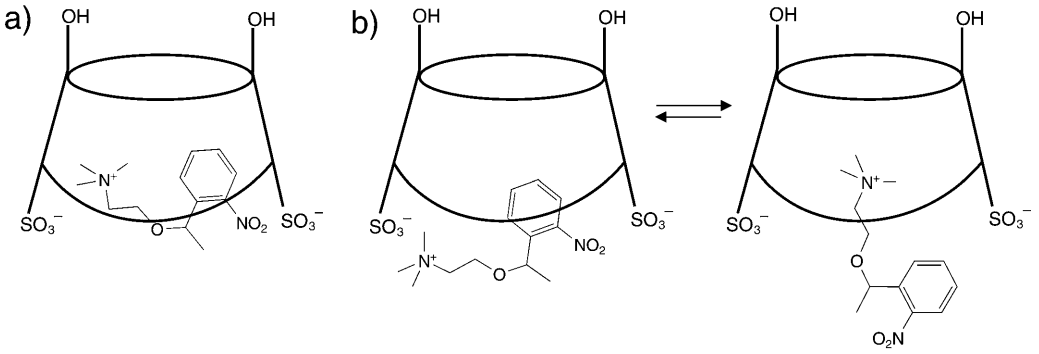

Fig. 8. *Two binding modes possibly involved in the formation of complex* [**A**-**3**]

Table 4. *^{1}H-NMR Maximum Upfield Chemical Shifts* ($\Delta\delta$, [ppm]) *and Dissociation constants* (K_D, [μM]) *of the Ammonium Moiety and the Aromatic Ring in* **A** *When Complexed with* **3** *in 100 mM Phosphate Buffer at Both pD 7.3 and pD 0.4*

pD	Me_3N^+		H–C(4) of Ar	
	$\Delta\delta_{max}$ [ppm]	K_D [μM]	$\Delta\delta_{max}$ [ppm]	K_D [μM]
7.3	1.01	29±10	0.55	24±10
0.4	0.75	28±15	1.10	32±8

chemical shift of the ammonium moiety and that of the aromatic H-atom in the *para*-position to the side chain. The fact that the complex [**A**-**3**] is not strongly dependent on the pH could not be explained by the binding mode shown in *Fig. 8,b*. It can also be assumed that the binding mode, shown in *Fig. 8,b*, for [**A**-**3**] could not explain the particularly strong binding characteristics observed for [**A**-**3**], albeit **3** has a very flexible character.

Based on the above results and our previous findings, we propose a ditopic binding mode (*Fig. 8,b*) for the complex [**A**-**3**]. In addition, this ditopic binding mode of [**A**-**3**] is consistent with the higher affinity observed, and the similar binding constants obtained for the ammonium and aromatic groups, regardless of the state of protonation of **3**. In addition, the ditopic binding of the ligand may displace H_2O molecules from the cavity, resulting in a favorable entropic gain. The ditopic binding of calix[8]arene was first observed in a study by *Shinkai et al.*, where two separate trimethylammonium functions were reported to bind into the cavity of the calix[8]arene in an 'induced-fit' manner [20].

We have previously reported, based on NOESY experiments and molecular-modeling studies, that the ditopic complex [**A**-**3**] was formed between the flexible ligand **A** and the flexible calix[8]arene (**3**) as the result of a 'mutually induced fitting' process [13]. Free ligand **A** is in an extended conformation according to its 3-D structure [11]. However, it adopts a bent conformation when complexed with **3** (*Fig. 9*), based on the NOESY experiments [13]. In the bent conformation, the ammonium moiety and the aromatic ring of **A** are brought closer to a distance of 4.0 Å so that they could be accomodated concomitantly in the cavity of **3** [13]. This suggests that the cav-

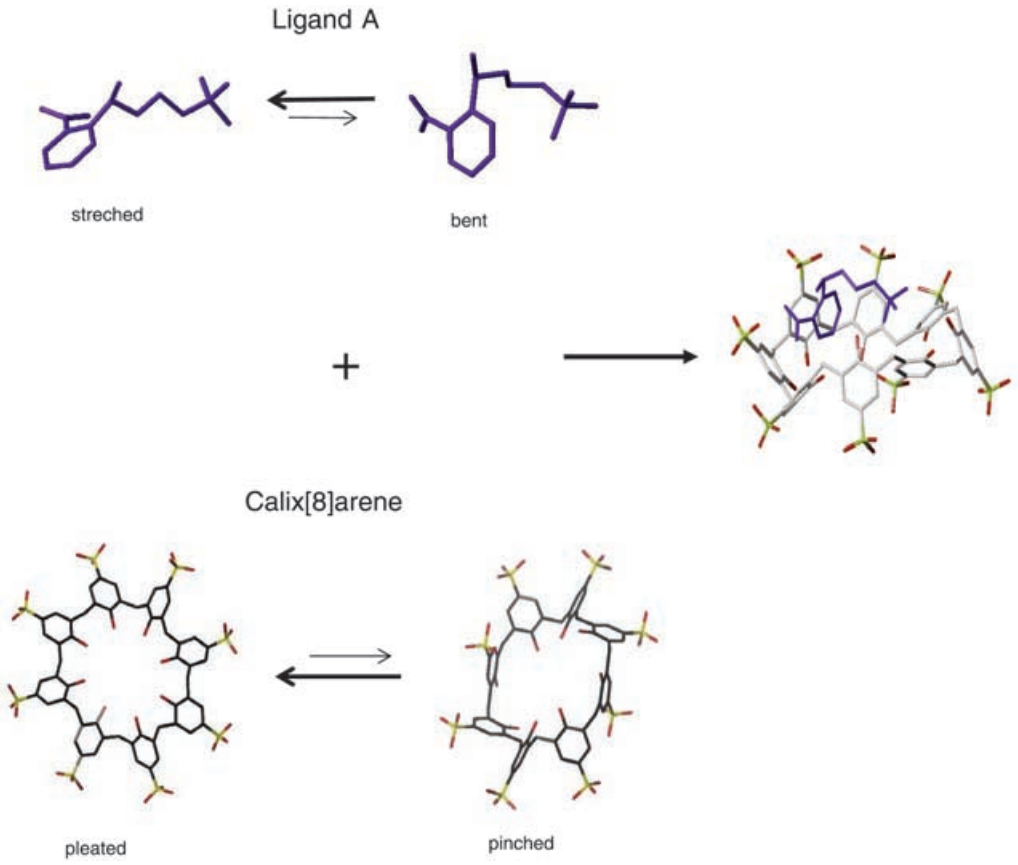

Fig. 9. *The complex* [**A**-**3**] *is formed* via *mutually induced fitting with the conformationally flexible guest and host molecules* **A** *and* **3**. When **A** and **3** are not complexed, **A** prefers the streched conformation (obtained from crystal structure [11]) to the bent conformation (from the NMR data [13]), while **3** prefers the pleated to the pinched conformations [13]. In the complex [**A**-**3**], **A** adopts the bent conformation and **3** the pinched conformation.

ity of **3** induces the flexible ligand **A** to adopt a bent conformation for a favorable fit in the complex [**A**-**3**]. Furthermore, **A** is also able to select a suitable conformation of **3** for a favorable binding, as suggested by molecular modeling studies reported in [13]. When **3** is free, the pleated loop conformation is preferred over the pinched one, with the former being by 10 kcal/mol lower in energy [13]. When **A** was docked in **3**, only a stable complex could be obtained selecting the pinched conformation of **3** and bent conformation of **A** [13]. Therefore, the complex [**A**-**3**] is formed *via* mutually induced fit between the conformationally flexible **A** and **3**, with both **A** and **3** adapting to each other, by selecting the higher-energy but appropriate geometric conformers for **A** to favorably fill the cavity of **3**. Furthermore, in the complex [**A**-**3**], the aromatic ring of **A** formed π–π interactions [21] with the phenol units of **3**, while the ammonium moiety of **A** formed a cation–π interactions with other phenol units of **3** in addition to the electrostatic interaction with the sulfonate group.

Conclusions. – In the present study, the water-soluble calixarenes **1**–**3** were investigated as synthetic receptors for photolabile cholinergic ligand **A**. All these calixarenes formed stable 1:1 complexes with **A**, and the dissociation constants of the various calixarene complexes ranged from 29 to 77 μM. The strongest interactions were observed with calix[8]arene (**3**), where the dissociation constants were similar to those observed with acetylcholinesterase (AChE) and butyrylcholinesterase (BuChE; *Table 3*), two important cholinergic enzymes. The high affinities of these calixarenes for **A** are comparable to those of the biological recognition sites in cholinesterases, suggesting that the *para*-sulfonated calixarenes mimick the binding sites of cholinesterases. Furthermore, the larger calix[8]arene (**3**) formed ditopic binding complexes by concomitantly binding to both the cholinergic moiety and the photolabile group of **A**, whereas the smaller calix[4]arene (**1**) and calix[6]arene (**2**) molecules formed monotopic complexes with **A** due to their small cavity size. The ditopic complex was formed between the flexible calix[8]arene (**3**) and the flexible ligand **A** *via* a 'mutually induced fitting' process, whereas the monotopic complexes between the calix[4]arene (**1**) and **A** may be regulated by the pH: at neutral pH, **1** specifically binds the cationic choline moiety, but at acidic pH, **1** unselectively hosts either the cationic choline moiety or the aromatic group of **A** in its cavity. Various modes of complexation were, therefore, found to be involved in the binding of the bifunctional molecule **A** in *para*-sulfonated calixarenes **1**–**3**, depending on their size, geometry, and state of protonation. In these complexes, the cooperative effects of electrostatic forces, hydrophobic effects, cation–π interactions, and the size and geometry of the molecules are all decisive binding factors. These calixarenes, therefore, constitute interesting examples of adaptive supramolecular biomimetic chemistry, and may open new perspectives for designing synthetic receptors.

Experimental Part

Reagents. The *para*-sulfonated calixarenes **1**–**3** were purchased from *Acros Organics*, and the photolabile cholinergic ligand **A** was prepared as reported earlier by *Peng* and *Goeldner* [7].

Mass-Spectroscopic Analysis. The binding complexes formed by calixarenes **1**–**3** with **A** in 0.05N ammonium carbonate at pH 7.2 with host/guest ratios of 1:1 and 1:3 were studied by electrospray mass spectrometry, operating in the positive-ion mode.

NMR Analyses. ^{1}H-NMR Spectra were recorded on *Bruker VPC 200* and *300* spectrometers when not specially mentioned.

Dissociation constants. Dissociation constants K_D were calculated from plots of ligand chemical shifts as a function of calixarene concentration [19]. Solns. for NMR titrations were prepared in deuterated 0.1M phosphate buffer at pD 7.3 or 0.4 at r.t., keeping the concentration of **A** (3.0×10^{-4} M) constant while varying that of the calixarene from 3.0×10^{-3} to 3.0×10^{-5} M.

Job's Plot. The stoichiometry of the complexes was determined from *Job*'s plots of the chemical shifts of the complexes *vs.* the molar fraction of **A**, keeping the sum of the total **A** and calixarene concentrations (6.0×10^{-4} M) constant while varying the molar fraction of **A** from 0 to 1.

DOSY. All the DOSY-NMR experiments were recorded with a *Bruker Avance* 500-MHz *Ultrashielded*™ spectrometer equipped with a pulsed gradient unit capable of producing magnetic field pulse gradients of 55 G·cm^{-1} in the *z*-direction. Samples for DOSY-NMR were prepared in deuterated 0.1M phosphate buffer, pD 7.3 at r.t. with **A** (5 mM) and the calixarene (5 mM). All spectra were acquired in a 5-mm inverse *Cryoprobe* at 300 K in 5-mm tubes. ^{1}H-NMR Spectra were obtained using a single-pulse sequence, and 16 scans were accumulated with a recycling time of 3 s. Chemical shifts were referred to TMS (0 ppm). All ^{1}H-DOSY-NMR experiments were performed using the Bipolar Pulse Longitudinal Eddy current Delay (BPLED) pulse sequence. The duration of the magnetic field pulse gradient (δ) and the diffusion time (Δ) were optimized for each sample in

order to obtain complete dephasing of the signals with the maximum gradient strength; typical values of 1.5–2.2 ms, and 100–200 ms, resp., were obtained. In each DOSY experiment, a series of 32 BPLED spectra on 32-K data points and 16 scans were collected. The pulse gradient strength (g) was increased from 2 to 95% of the maximum, in a quadratic ramp. After *Fourier* transformation of the F2 dimension, the diffusion dimension was processed with the *Bruker* XWIN-NMR software package (version 3.1). Assuming the complexes to be spherical molecules, the estimated molecular weights of the complexes were deduced from the following equation [16]:

$$\frac{D_1}{D_2} = \sqrt[3]{\frac{M_2}{M_1}}$$

NOESY. Solns. for NOESY-NMR analysis were prepared with 20 mM of **A** and 40 mM of the host, which ensured over 99% complex formation between the guest and the host. 2D-NMR Spectra were recorded by using a NOESY sequence from *Bruker* (*Noesyprtp*) [22] and a mixing time of 400 ms. We conducted the experiments on **A**, [**A**-**1**], and [**A**-**3**], respectively.

Molecular Modeling. The starting structure **A** was constructed from the coordinates of the crystal structure of an analog [11]. For **3**, two crystal structures of calix[8]arene, *Dovhif* [23] and *Foztix* [24], were used as starting point to construct the structure, leading to the pleated loop conformation and the pinched conformation, respectively. For the complex [**A**-**3**], **A** was manually docked with each conformer of **3**. All the starting structures of **A**, **3**, and [**A**-**3**], were optimized by molecular-mechanics algorithm using the *Tripos Force Field* [25] with a convergence criterion of 0.01 kcal/mol. The electrostatic component was applied by means of the *Gasteiger–Hückel* charges and a dielectric function equal to 1.

This work was supported by the *CNRS*, the *COST* program *D11*, the *Région Alsace*, and by the *EU Biotechnology* program No. 960081. We thank Prof. *Alain van Dorsselaer* and Dr. *Helene Niergarten* for MS experiments. We are grateful to Prof. *S. Caldarelli* and to *S. Viel* for helpful suggestions about the DOSY experiments. We thank Drs. *Viveka Vadyvaloo* and *Alain Méou* for helping to improve the paper, and Dr. *Jessica Blanc* for the final revision of the English manuscript.

REFERENCES

[1] J. M. Lehn, 'Supramolecular chemistry: Concepts and perspectives', VCH, Weinheim, 1995; S. H. Gellman, Guest Ed., 'Molecular recognition', *Chem. Rev.* **1997**, *97*, 1231–1734; 'Supramolecular Chemistry and Self-assembly Special Feature', Ed. J. Halpern, *Proc. Natl. Acad. Sci. U.S.A.* **2002**, *99*, 4763–5206.
[2] C. D. Gutsche, 'Calixarene', Royal Society of Chemistry, Cambridge, 1989; C. D. Gutsche, 'Calixarene revisited', Royal Society of Chemistry, Cambridge, 1998; 'Topics in inclusion science, Vol 3: Calixarenes: A versatile class of macrocyclic compounds', Eds. J. Vicens, V. Böhmer, Kluwer, Dordrecht, 1991; V. Böhmer, *Angew. Chem., Int. Ed*. **1995**, *34*, 713; 'Calixarene 2001', Eds. Z. Asfari, V. Böhmer, J. Harrowfield, J. Vicens, Kluwer, Dordrecht, 2001.
[3] A. Ikeda, S. Shinkai, *Chem. Rev.* **1997**, *97*, 1713; F. Sansone, L. Baldini, A. Casnati, M. Lazzarotto, F. Ugozzoli, R. Ungaro, *Proc. Natl. Acad. Sci. U.S.A*. **2002**, *99*, 4842; J. Rebek, *Chem. Commun.* **2000**, 637.
[4] J. M. Lehn, R. Méric, J.-P. Vigneron, M. Cesario, J. Guilhem, C. Pascard, Z. Asfari, J. Vicens, *J. Supramol. Chem.* **1995**, *5*, 97.
[5] K. N. Koh, K. Araki, A. Ikeda, H. Otsuka, S. Shinkai, *J. Am. Chem. Soc.* **1996**, *118*, 755.
[6] D. A. Dougherty, *Science*, **1996**, *271*, 163; J. C. Ma, D. A. Dougherty, *Chem. Rev.* **1997**, *97*, 1303; N. Zacharias, D. A. Dougherty, *Trends Pharmacol. Sci.* **2002**, *23*, 281.
[7] L. Peng, M. Goeldner, *J. Org. Chem.* **1996**, *61*, 185.
[8] L. Peng, I. Silman, J. Sussman, M. Goeldner, *Biochemistry* **1996**, *35*, 10854; L. Peng, C. Colas, M. Goeldner, *Pure Appl. Chem.* **1997**, *69*, 755; L. Peng, M. Goeldner, *Methods Enzymol.* **1998**, *291*, 265.
[9] L. Peng, J. Wirz, M. Goeldner, *Angew. Chem., Int. Ed.* **1997**, *36*, 398.
[10] L. Peng, J. Wirz, M. Goeldner, *Tetrahedron Lett.* **1997**, *38*, 2961.
[11] L. Peng, F. Nachon, J. Wirz, M. Goeldner, *Angew. Chem., Int. Ed.* **1998**, *37*, 2691.
[12] A. Specht, J. Wirz, M. Goeldner, L. Peng, *Synlett* **1999**, *SI*, 981.
[13] A. Specht, P. Bernard, M. Goeldner, L. Peng, *Angew. Chem., Int. Ed.* **2002**, *41*, 4706.
[14] C. S. Johnson, *Prog. Nucl. Magn. Reson. Spectrosc.* **1999**, *34*, 203.

[15] M. Bergamaschi, F. Bigi, M. Lanfranchi, R. Maggi, A. Pastorio, M. A. Pellinghelli, F. Peri, C. Porta, G. Sartori, *Tetrahedron* **1997**, 53, 13037.
[16] A. R. Waldeck, P. W. Kuchel, A. J. Lennon, B. E. Chapman, *Prog. Nucl. Magn. Reson. Spectrosc.* **1997**, *30*, 39.
[17] G. Arena, A. Casnati, A. Contino, G. G. Lombardo, D. Sciotto, R. Ungaro, *Chem.–Eur. J.* **1999**, *5*, 738; G. Arena, A. Casnati, A. Contino, R. G. Gulino, D. Sciotto, R. Ungaro, *J. Chem. Soc., Perkin Trans. 2* **2000**, *5*, 419.
[18] S. Shinkai, K. T. Araki, Mutsuda, N. Nishiyama, H. Ikeda, I. Takasu, M. Iwamoto, *J. Am. Chem. Soc.* **1990**, *112*, 9053.
[19] H.-J. Schneider, H. Dürr, Ed. 'Frontiers in supramolecular organic chemistry and photochemistry', VCH, Weinheim, 1991, p. 123–143.
[20] S. Shinkai, K. Araki, O. Manabe, *J. Am. Chem. Soc.* **1988**, *110*, 7214.
[21] E. A. Meyer, R. K. Castellano, F. Diederich, *Angew. Chem., Int. Ed.* **2003**, *42*, 1210.
[22] J. Jeener, B. H. Meier, P. Bachmann, R. R. Ernst, *J. Chem. Phys.* **1979**, *71*, 4546.
[23] C. D. Gutsche, A. E. Gutsche, A. I. J. Karoulov, *J. Inclusion Phenom.* **1985**, *3*, 447.
[24] A. W. Coleman, S. G. Bott, J. L. Atwood, *J. Inclusion Phenom.* **1987**, *5*, 581.
[25] SYBYL Molecular Modeling System, v. 6.62, *Tripos Associates*, St. Louis, MO, 2000.

Received May 3, 2005